Research
Microecology—Article

Functional Metabolomics Reveals that *Astragalus* Polysaccharides Improve Lipids Metabolism through Microbial Metabolite 2-Hydroxybutyric Acid in Obese Mice

Bingbing Li [a,#], Ying Hong [a,#], Yu Gu [a], Shengjie Ye [a], Kaili Hu [a], Jian Yao [b], Kan Ding [b], Aihua Zhao [c], Wei Jia [c,d], Houkai Li [a,*]

[a] *Institute of Interdisciplinary Integrative Medicine Research, Shanghai University of Traditional Chinese Medicine, Shanghai 201203, China*
[b] *Shanghai Institute of Materia Medica, Chinese Academy of Sciences, Shanghai 201203, China*
[c] *Shanghai Key Laboratory of Diabetes Mellitus and Center for Translational Medicine, Shanghai Jiao Tong University Affiliated Sixth People's Hospital, Shanghai 200233, China*
[d] *University of Hawaii Cancer Center, Honolulu, HI 96813, USA*

ARTICLE INFO

ABSTRACT

Polysaccharides are widely present in herbs with multiple activities, especially immunity regulation and metabolic benefits for metabolic disorders. However, the underlying mechanisms are not well understood. Functional metabolomics is increasingly used to investigate systemic effects on the host by identifying metabolites with particular functions. This study explores the mechanisms underlying the metabolic benefits of *Astragalus* polysaccharides (APS) by adopting a functional metabolomics strategy. The effects of APS were determined in eight-week high-fat diet (HFD)-fed obese mice. Then, gas chromatography–time-of-flight mass spectrometry (GC–TOFMS)-based untargeted metabolomics was performed for an analysis of serum and liver tissues, and liquid chromatography–tandem mass spectrometry (LC–MS/MS)-based targeted metabolomics was performed. The potential functions of the metabolites were tested with *in vitro* and *in vivo* models of metabolic disorders. Our results first confirmed the metabolic benefits of APS in obese mice. Then, metabolomics analysis revealed that APS supplementation reversed the HFD-induced metabolic changes, and identified 2-hydroxybutyric acid (2-HB) as a potential functional metabolite for APS activity that was significantly decreased by a HFD and reversed by APS. Further study indicated that 2-HB inhibited oleic acid (OA)-induced triglyceride (TG) accumulation. It was also found to stimulate the expression of proteins in lipid degradation in hepatocytes and TG lipolysis in 3T3-L1 cells. Moreover, it was found to reduce serum TG and regulate the proteins involved in lipid degradation in high-fat and high-sucrose (HFHS)-fed mice. In conclusion, our study demonstrates that the metabolic benefits of APS are at least partially due to 2-HB generation, which modulated lipid metabolism both *in vitro* and *in vivo*. Our results also highlight that functional metabolomics is practical for investigating the mechanism underlying the systemic benefits of plant polysaccharides.

1. Introduction

Obesity is the basis for most metabolic disorders characterized by dysregulated lipids metabolism, inflammation, and insulin (INS) resistance [1–5]. Excessive energy intake or activated *de novo* synthesis of fatty acids accelerates the development of obesity and obesity-related metabolic disorders [6,7]. Over 1.9 billion adults in the world are overweight [8]. Unfortunately, very few options are available for body weight reduction with sufficient safety and effectiveness [9].

Traditional Chinese medicine (TCM) has been practiced in China and other Asian countries for thousands of years [10]. Herb-derived polysaccharides are a class of active macromolecules with multiple benefits for maintaining health and for disease prevention [11]. Recently, Chang et al. [12] and Wu et al. [13] reported that polysaccharides extracted from *Ganoderma lucidum* and *Hirsutella sinensis* exhibited an obvious anti-obesity effect in high-fat diet (HFD)-fed mice. *Astragalus membranaceus* is the medicinal part of

the dry root of *Astragalus* (Fisch.) Bge. or *Astragalus membranaceus* (Fisch.) Bge. var. *mongholicus* (Bge.) Hsiao [14]. *Astragalus membranaceus* is widely used in TCM for improving immunity, and as a dietary supplement [15]. *Astragalus* polysaccharides (APS) are extracted from *Astragalus membranaceus* and show well-established benefits in mice with metabolic disorders [16–18]. Our recent study indicated that APS is also effective in attenuating obesity and modulating the gut microbiota in HFD-fed mice [19]. However, the underlying mechanism of APS is not clear.

Metabolomics is an omics approach for monitoring the metabolic status of the host under pathophysiological conditions by measuring the relative or absolute levels of metabolites in biological samples such as blood, urine, feces, or tissues [20]. Increasing evidence has demonstrated that many endogenous metabolites are not only the readouts of host or gut microbiota, but also molecules with potent functions for host energy metabolism such as itaconate, short-chain fatty acids, and bile acids [21–23]. As a result, functional metabolomics is emerging as an important strategy to investigate the potential biological functions of identified metabolites in disease formation or treatment based on untargeted or targeted metabolomics.

In this study, we adopted an untargeted and targeted metabolomics approach to investigate the mechanisms underlying the metabolic benefits of APS in HFD-fed obese mice. Our results confirmed that APS is effective in attenuating body weight gain and obese-related disorders. We then identified dozens of differential metabolites that were significantly altered in either HFD or APS-supplemented mice in serum and liver tissues, which were subjected to further testing of their biological functions in lipids metabolism. We determined that 2-hydroxbutyric acid (2-HB), a bacteria-related metabolite, was reversely altered by APS supplementation, which was effective in improving lipids metabolism both *in vitro* and *in vivo*.

2. Materials and methods

2.1. Cell culture

All cells used in this research were provided by the Institute of Biosciences Cell Resource Center, Chinese Academy of Sciences, Shanghai, China. HepG2, RAW264.7, and 3T3-L1 cells before and after differentiation were cultured in a basic medium—that is, Dulbecco's modified Eagle's medium (DMEM; Gibco, USA) containing 10% fetal bovine serum (FBS; Gibco), penicillin (200 units·mL^{-1}), and streptomycin (200 mg·mL^{-1}). AML12 cells were cultured in DMEM/nutrient mixture F-12 (DMEM/F-12; Invitrogen, USA) supplemented with 10% (v/v) heat-inactivated FBS, 1% insulin transferrin selenium (ITS) liquid media supplement (100×; Sigma-Aldrich, USA), dexamethasone (40 ng·mL^{-1}; Sigma-Aldrich), sodium bicarbonate (1.2 g·L^{-1}), penicillin (200 units·mL^{-1}), and streptomycin (200 mg·mL^{-1}). All cells were cultured in a humidified cell culture CO_2 incubator (Esco Micro Pte. Ltd., Singapore) at 37 °C and 5% CO_2.

2.1.1. INS resistance model

HepG2 cells were seeded into 12-well plates at a density of about 1.25×10^5 cells·cm^{-2} and the medium was changed every 24 h for 2 d after seeding until the culture reached approximately 80% confluence. For the INS resistance model, 2.5 mmol·L^{-1} of glucosamine (GS; Shanghai Biyuntian Biotechnology Co., Ltd., China) was added for 18 h without FBS, the medium was then changed to 10% FBS DMEM with the presence of GS and 2-HB (Sigma-Aldrich). After 24 h, the cells were treated for 20 min with INS (ganshulin recombinant human INS injection). Finally, the cells were collected and protein was extracted for subsequent determination.

2.1.2. Lipid aggregation model

AML12 cells were seeded into 24-well plates at a density of about 1.25×10^5 cells·cm^{-2}. The medium was changed every 24 h until the culture reached approximately 80% confluence. For the lipid aggregation model, the cells were treated for 24 h with 0.2 mmol·L^{-1} oleic acid (OA; Sigma-Aldrich), or different doses of 2-HB were added. Then the cells were collected for subsequent determination.

2.1.3. Inflammation model

RAW264.7 cells were seeded into 24-well plates at a density of 4.0×10^5 cells·cm^{-2} and the culture medium was changed every 24 h. For the inflammation model, cells were first treated with different doses of 2-HB for 0.5 h; they were then stimulated with 100 ng·mL^{-1} lipopolysaccharide (LPS; Sigma-Aldrich) for 4 h. Finally, the cells were collected and message RNA (mRNA) was extracted for the determination of mRNA content.

2.1.4. Adipocyte culture and treatment

3T3-L1 cells were seeded into six-well plates, and the medium was changed every 24 h. After contact inhibition for 48 h, differentiation solution was added to promote cell differentiation into adipocytes. First, the medium was changed to differentiation medium A, which contained high-glucose DMEM, 10% (v/v) heat-inactivated FBS, INS (10 mg·L^{-1}), dexamethasone (1 µmol·L^{-1}), and isobutyl methylxanthine (IBMX) (0.5 mmol·L^{-1}). After 48 h, the medium was changed to differentiation medium B, which contained high-glucose DMEM, 10% (v/v) heat-inactivated FBS, and INS (10 mg·L^{-1}). After 48 h, the medium was changed to 0% FBS DMEM. The cells were cultured in the basic medium for 6–8 d, and the medium was changed every 48 h. The cells were then observed under a microscope. If the cell morphology was round and there were yellow lipid droplets in the cells, then the differentiation was successful. The cells were treated with 2-HB for 24 h, and then collected for subsequent determination.

2.2. Extraction method of APS

In this study, APS was extracted from *Astragalus membranaceus* (Shanghai Kangqiao Chinese Medicine Tablet Co., Ltd., China) using a well-established polysaccharide extraction method involving water extraction and alcohol precipitation [24]. To summarize, distilled water was added to the *Astragalus membranaceus* with the volume of ten times, eight times and six times, respectively, and each mixture was decocted for one hour. The three filtrated decoctions were then combined and concentrated to a third of the volume at a temperature less than 60 °C. Ethanol was then added up to 70% and precipitated overnight. Next, the precipitate was dried under vacuum at a temperature less than 60 °C.

2.3. Characterization of the monosaccharide composition of APS

The extracted APS was hydrolyzed into monosaccharides with trifluoroacetic acid (TFA), and the hydrolyzed monosaccharides from APS along with authentic monosaccharide standards were then acetylated according to a previously reported method [25]. After that, the acetylated samples were analyzed using a 7890B gas chromatograph (Agilent Technologies, USA) equipped with a 3% OV-225/AW-DMCS-Chromosorb W column (3 mm × 2.5 m; Shimadzu Global Laboratory Consumables Co., Ltd., Japan). The heating program for the gas chromatography (GC) analysis was as follows: The initial temperature was 140 °C. The temperature was then increased to 198 °C at a rate of 2 °C·min^{-1} and maintained for 4 min. Next, it was increased to 214 °C with a temperature gradient of 4 °C·min^{-1}, and then increased to 217 °C at a speed of 1 °C·min^{-1} and maintained for 4 min. Finally, the temperature

was increased to 250 °C at the rate of 3 °C·min^{-1} and held constant for 5 min. The component determination result is shown in Appendix A Fig. S1. The APS used in this study was found to be composed of five monosaccharides: rhamnose (1.60%), arabinose (23.39%), xylose (0.84%), glucose (70.55%), and galactose (3.61%).

2.4. Animal experimentation

All the mice used in the experiments were four weeks old when they were purchased from Laboratory Animal Center (Shanghai, China). They were housed in a regulated barrier system facility at 23–24 °C with 60% ± 10% relative humidity and a 12 h light/dark cycle. After a week of adaptation, all mice were randomly divided into different groups for the experiments. All the animal experiments were approved by the Animal Experiment Institution of Shanghai University of Traditional Chinese Medicine (Shanghai, China), and the protocol was approved by the Institutional Animal Ethics Committee.

The APS administration experiment was carried out as follows. Male C57BL/6J mice (four weeks old) were treated with a chow diet (control; Jiangsu Cooperative Pharmaceutical Bioengineering Co., Ltd., China) or an HFD (D12492; Research Diets Inc., USA) with or without APS supplementation (4% APS in HFD) for eight weeks (HFD, APS).

The 2-HB administration experiments were carried out as follows. Mice were divided into three groups: a control group fed a chow diet, a high-fat and high-sucrose (HFHS) group fed an HFD and 30% sucrose added in drinking water, and a 2-HB group fed an HFHS diet along with oral gavage of 2-HB (0.01 mL·g^{-1} body weight) daily for two weeks at a dosage of 250 mg·kg^{-1} body weight. For the 2-HB injection administration experiment, the mice had been fed with chow or an HFHS diet for eight weeks prior to the two weeks of 2-HB administration (250 mg·kg^{-1} body weight, intraperitoneal injection). The 2-HB solution was prepared with phosphate buffered saline (PBS) at 25 mg·mL^{-1}. Finally, the mice were sacrificed after anesthesia with 10% chloral hydrate intraperitoneally in order to collect the liver and white adipose tissues, blood, and cecum contents after overnight fasting (16 h). Serum samples were obtained by centrifuging blood at 4000 r·min^{-1} at 4 °C (5424R; Eppendorf, Germany). Part of the liver and white adipose tissues were fixed with 10% formalin; other tissues were quickly frozen in liquid nitrogen and then stored at −80 °C (New Brunswick Science U570-86; Eppendorf).

2.5. Triglyceride content determination

To determine the intracellular triglyceride (TG) content, the cells were washed twice with 4 °C pre-cooled PBS, and a considerable amount of lysis solution (Shanghai Biyuntian Biotechnology Co., Ltd.) was added for the complete lysis of proteins. The scraped cells were placed in a 1.5 mL Eppendorf micro test (EP) tube, and magnetic beads added in a grinding machine (BiHeng Biotechnology Inc., China) for grinding. 2.5 μL of the mixed cell lysate was taken out from the EP tube and added to a 96-well plate; 200 μL of the working solution (Nanjing Jiancheng Bioengineering Institute, China) was added thereto. The 96-well plate was incubated in an oven at 37 °C for 10 min (Shanghai Fuma Laboratory Instrument Co., Ltd., China). The absorbance of reaction mixture was then measured at 510 nm using a microplate reader (SPARK 10 M; TECAN, Switzerland). The remaining mixed cell lysates were centrifuged at 13 000 r·min^{-1} for 10 min at 4 °C. The supernatant was then taken and the protein concentration was determined by means of the bicinchoninic acid (BCA) method (Thermo Fisher Scientific (China) Co., Ltd., China). Protein concentration was used to correct the TG content.

2.6. Protein analysis

Snap-frozen tissues and treated cells were added to the appropriate lysate, ground with magnetic beads, and centrifuged at 12 000 r·min^{-1} for 10 min at 4 °C. The supernatant was then taken to determine the protein concentration by means of the BCA method. For Western blotting, the protein concentration was adjusted and a loading buffer (Shanghai Biyuntian Biotechnology Co., Ltd.) was added. Next, each of the mixture was heated at 100 °C for 10 min; after that, it was allowed to cool naturally. Equal amounts of proteins were separated on concentration gel at a voltage of 80 or 120 V (Bio-Rad Laboratories, Inc., USA). The current was fixed at 380 mA during membrane transfer, and the transfer time was adjusted according to the molecular weight. Next, the proteins were transferred onto polyvinylidene fluoride (PVDF) membranes. The PVDF membranes were sealed for 90 min using 5% skimmed milk. An antibody was then added and each mixture was left overnight at 4 °C on an orbital shaker (Haimen Kylin-Bell Lab Instruments Co., Ltd., China). The blots were then reacted with Horseradish peroxidase (HRP)-linked anti-rabbit immunoglobulin G (IgG) or anti-mouse IgG, followed by enhanced chemiluminescence (Shanghai Biyuntian Biotechnology Co., Ltd.). Information about the antibodies is provided in Appendix A Table S1.

2.7. Oil red staining

The treated cells were washed twice with pre-cooled PBS; next, 10% neutral formalin (Sinopharm Chemical Reagent Co., Ltd., China) was added and the mixture was left for 30 min. Oil red (Sigma-Aldrich) was then added and the mixture was left for 15 min. The oil red contained 40% pure water (Millipore). After mixing, the oil red was filtered using a microporous membrane. Next, filtered hematoxylin (Sigma-Aldrich) was added and the mixture was left for 7 min. Finally, the cells were washed with PBS.

2.8. Quantitative real-time polymerase chain reaction analysis

Trizol (Thermo Fisher Scientific (China) Co., Ltd.) was used to extract RNA from cells or tissues and reverse the RNA to complementary DNA (cDNA) with a one-step method according to the kit procedure. Next, the primers of the target genes were added to the cDNA samples. The mixture of cDNA, polymerase chain reaction (PCR) master mix (YEASEN, China) and water was performed for PCR amplification (Bio-Rad Laboratories, Inc.). The primer sequences of the genes are provided in Appendix A Table S2.

2.9. Untargeted metabolomics analysis

The extracted samples were analyzed to obtain global metabolite profiles using an untargeted metabolic profiling platform, the XploreMET™ (Metabo-Profile, China), measured by a time-of-flight mass spectrometer (TOFMS; Leco, USA) with GC (Agilent) and a robotic online derivatization station. Raw data were processed in XploreMET to determine the ion peaks, followed by denoising baseline correction. State-of-the-art GC–TOFMS technology with fast scan rates can resolve hundreds of metabolite peaks with a deconvolution algorithm in a single injection. A typical GC–TOFMS chromatogram of biological samples generates 600–1000 individual deconvoluted signals. However, molecules containing multiple reactive groups (i.e., OH, NH, SH, and NH$_2$) may form multiple (oxime) tetramethyl silane (TMS) derivatives and produce multiple derivatives for the same metabolite. XploreMET identifies all of the TMS derivatives using the knowledge of an existing database, JiaLib™ 1500+ (Metabo-Profile), which was built from the pure chemical standard; calculates the sum of the derivatives;

and reports it as a single annotated metabolite for the same metabolite. The ratios of the two adjacent metabolites were calculated from the known metabolic relation network (Kyoto Encyclopedia of Genes and Genomes (KEGG)). XploreMET used the score values of one model dimension (t1, t2, etc.) from a multivariate model—in this case, within a principal component analysis (PCA) as the control chart y-variable—and yielded a multivariate control chart (MCC) based on the combination of all the x-variables—that is, the metabolite signals. Hence, the MCC displays the data which has been measured on the process over time and can monitor variations produced by a series of laboratory procedures. In the determination process, all the actual samples were within the control limits and fluctuated beyond and below the x-axis, while the quality control (QC) samples were separated from the actual samples. More details have been described in a previous publication [26].

2.10. Targeted metabolomics analysis

Methanol was used to remove the protein from the serum samples and liver samples, and the supernatant after centrifugation was determined by means of liquid chromatography–tandem mass spectrometry (LC–MS/MS). The analysis was carried out using high-performance liquid chromatography (HPLC; Shimadzu Global Laboratory Consumables Co., Ltd.) coupled with an AB SCIEX 4500 (USA). Gradient elution was used at 0.3 mL·min^{-1} with acetonitrile as the organic phase and 0.1% formic acid as the water phase. The proportion of the organic phase was 3% in the first 0.8 min; it then increased to 50% at 0.9 min and maintained for 0.6 min. Finally, keep the proportion of organic phase in 3% over a period of 1.6–3.0 min. The injection volume was 1 μL. Electrospray was performed using the negative ionization mode. An ion spray voltage of −4500 V, a heated nebulizer temperature of 550 °C, and curtain gas (N_2), nebulizing gas (N_2), and heater gas (N_2) pressures of 275.800, 379.225, and 413.700 kPa, respectively, were set for the quantification of the precursor to product ion transitions in multiple reaction monitoring (MRM) mode. The Q1 mass/Q3 mass for 2-HB was 103.0/57.1. Medium collision-activated dissociation (CAD) and −16 V collision energy (CE), −8 V collision cell exit potential (CXP), −10 V entrance potential (EP), and −44 V declustering potential (DP) were used for the analysis. The linear range was 15.625–1000.000 ng·mL^{-1}, and the dwell was 650 ms. For 2-HB with a confirmed identity, the corresponding peak in the ion chromatogram was integrated using MultiQuant v.2.1 (AB SCIEX) to determine the area under the curve (AUC). For comparisons of metabolite levels between samples, data were calculated based on the AUC values, normalized to the corresponding liver weight. The extracted ion chromatograms (XIC) of 2-HB at the [M−H] ion are shown in Appendix A Fig. S2.

2.11. Pathway analysis

First, we entered the names of all 24 differential metabolites in MetaboAnalyst†. Next, we selected Fisher's exact test for pathway enrichment analysis and out-degree centrality for pathway topology analysis. The p values were obtained by pathway enrichment analysis, while pathway impact values were obtained by pathway topology analysis. All of the analysis was based on the KEGG version pathway library. The metabolome view shows all matched pathways according to the p values and pathway impact values (for more information, see Appendix A Table S3). We then chose the important pathways on the basis of the p values and pathway impacts.

---

† https://www.metaboanalyst.ca/MetaboAnalyst/home.xhtml.

2.12. Statistical analysis

Data are shown as means ± standard error of mean (SEM) unless otherwise noted. Statistical significance was determined with the unpaired two-tailed Student's t-test. A $p < 0.05$ was considered to be statistically significant.

3. Results

### 3.1. APS inhibits body weight gain and hepatic steatosis in HFD-fed mice

Male C57BL/6J mice were fed with either a normal chow diet or an HFD with or without APS supplementation for eight weeks. First of all, we found that the body weight of the mice in HFD group was significantly heavier than those in the control group, and was reduced by APS supplementation during the experiment. In addition, APS supplementation attenuated the HFD-induced metabolic phenotypes, including the TG contents in liver tissues, the weight and index of white adipose tissues (WAT), the degree of hepatic steatosis, and the volume of adipocytes (Fig. 1). The results indicated that APS supplementation attenuated metabolic disorders in HFD-fed obese mice.

3.2. Untargeted and targeted metabolomic analysis on serum and liver tissues

Given the non-absorptivity of most herbal polysaccharides, we speculated whether the metabolic benefits of APS were associated with the modulation of the endogenous metabolism. We therefore performed GC–TOFMS-based untargeted metabolomics on both the serum and liver tissues of mice. In general, a total of 166 and 112 metabolites, respectively, were determined in the serum and liver tissues. The alteration of these metabolites among groups were visualized with heatmaps (Appendix A Figs. S3 and S4). The 166 determined metabolites in the serum samples were composed of 34% amino acids, 18% carbohydrates, 14% organic acids, 12% fatty acids, 7% nucleotides, 5% lipids, 3% indoles, and 7% others, while the 112 metabolites in liver tissues contained 26% amino acids, 21% carbohydrates, 18% organic acids, 14% fatty acids, 8% nucleotides, 4% lipids, and 9% others. PCA was then conducted on the basis of these metabolites in serum or liver tissues. Clear separation was consistently observed among the groups, with 53.1% and 41.4% interpretation powers, respectively (Figs. 2(a) and (b)). The accumulated R^2X of the two PCA models were 0.531 and 0.413, while the Q^2 were 0.347 and 0.105, respectively. These results suggested that APS supplementation dramatically altered the metabolic profiles of the serum and liver tissue of HFD-fed mice.

Next, we screened the differential metabolites in the serum and liver tissues among the groups with the double criteria of variable importance for the projection (VIP) > 1 and $p < 0.05$ in multivariate and univariate statistical analysis simultaneously. A total of 18 and 6 differential metabolites and ratios of metabolites were identified in serum or liver tissues, respectively, which were reversely altered by HFD and APS (Figs. 2(c) and (d)). The 18 differential metabolites within the serum included ten amino acids and amino acid ratios (including 2-HB, dimethylglycine, β-alanine, citrulline, lysine, β-alanine/aspartic ratio, citrulline/arginine ratio, allantoic acid, urea, and 1-tyrosine/phenylalanine ratio), four fatty acids (including linoleic acid, OA, myristic acid, and dodecanoic acid), and four other metabolites (including 3-indolepropionic acid (IPA), inositol, myoinositol, and galactonic acid). The 6 differential metabolites within the liver tissues were 2-HB, α-aminobutyric acid, ornithine, arachidonic acid, arachidic acid, and docosahexaenoic acid. The
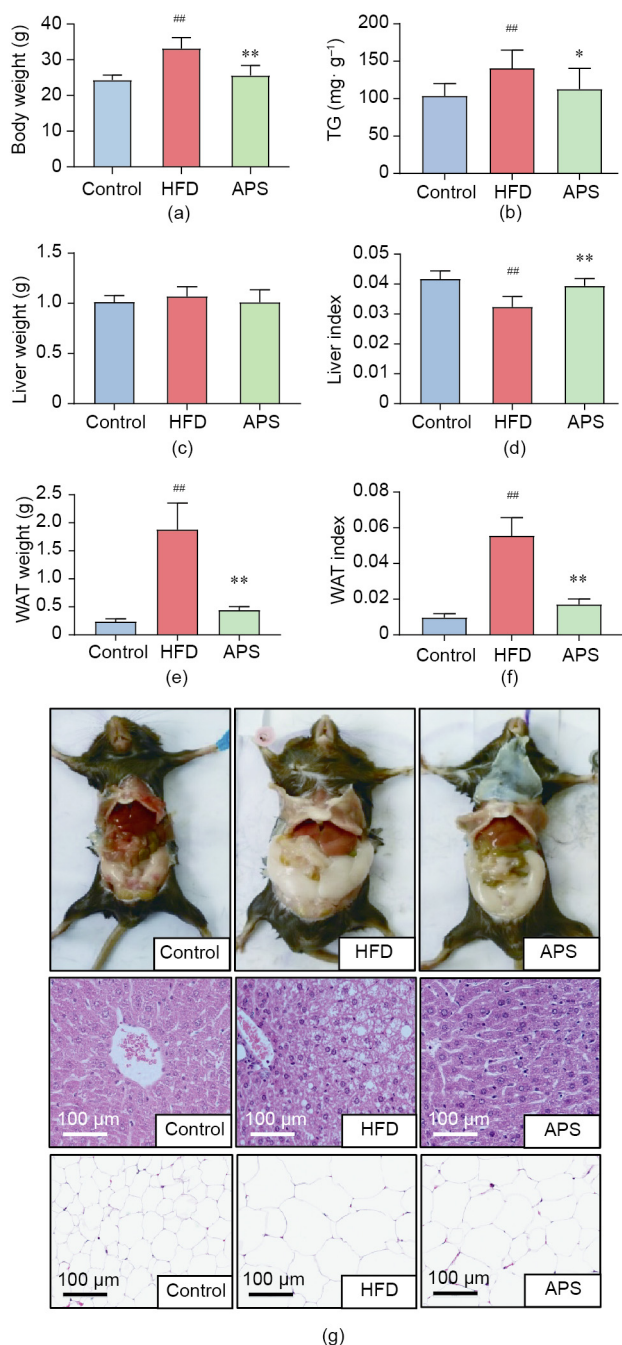
Fig. 1. APS attenuates hepatic steatosis and WAT lipid accumulation in HFD-fed mice. Male C57BL/6J mice (four weeks old) were treated with a chow diet (control) or HFD with or without 4% APS supplementation for eight weeks. (a) Body weight at the end of the experiment (n = 9, 10, and 10 per group). (b) Hepatic TG levels (n = 8, 9, and 8 per group). (c) Liver weight (n = 9, 10, and 10 per group). (d) Liver index (n = 9, 10, and 10 per group). (e) WAT weight (n = 9 per group). (f) WAT index (n = 9 per group). (g) Mice body, representative photomicrographs of liver tissues with hematoxylin eosin (HE) staining, and representative photomicrographs of WAT with HE staining (n = 3 per group). Significance was measured by an unpaired two-tailed Student's t-test, with $^{##}p < 0.01$ compared with the control group, and $^*p < 0.05$ and $^{**}p < 0.01$ compared with HFD group. Results are presented as means ± SEM.

metabolic pathway and functional analysis were then performed with these 24 (18 in serum and 6 in liver tissues) metabolites together. Four key metabolic pathways were enriched: the pathways of arginine and proline metabolism, propanoate metabolism, ascorbate and aldarate metabolism, and linoleic acid metabolism

(Figs. 2(e) and (f)). Based on the well-established functions of short-chain fatty acids in metabolic diseases [27], we focused on the altered propanoate metabolism pathway [28–49], in which 2-HB was consistently altered in both serum and liver tissues by APS supplementation (Fig. 2(g), Appendix A Tables S3 and S4). Next, the 2-HB contents in both serum and liver tissues were quantified with targeted metabolomics. The results showed that 2-HB was consistently reduced in the HFD group, and was reversed by APS supplementation (Figs. 2(h) and (i)). These results suggested that APS supplementation could reverse the metabolic alteration in serum and liver tissues in HFD-fed mice.

3.3. 2-HB regulates lipids metabolism, improves insulin sensitivity, and inhibits inflammation in vitro

To test whether the metabolic benefits of APS were associated with the increased production of 2-HB in mice, we first explored the effects of 2-HB on lipids metabolism in both hepatocytes and adipocytes. An OA-induced TG accumulation model was built in AML12 cells with obvious lipid droplets and a clear increase in cellular TG levels. 2-HB (0.1–10.0 mmol·L^{-1}) intervention significantly reduced OA-induced TG accumulation and improved cell viability at 10 mmol·L^{-1} concentration (Figs. 3(a)–(c)). Moreover, we observed that 2-HB treatment stimulated the expression of adipose triglyceride lipase (ATGL), hormone-sensitive lipase (HSL), and carboxylesterase 1 (CE1) proteins in AML12 cells (Figs. 3(d)–(h)), which suggested that 2-HB stimulated lipolysis [50–52]. In addition, 2-HB increased the expression of ATGL protein and the release of glycerin in 3T3-L1 cells (Figs. 3(i)–(k)).

Along with disordered fatty acid metabolism, inflammation and INS resistance are important risk factors of metabolic disorders [53]. To test whether 2-HB could attenuate inflammation and INS resistance, macrophage RAW264.7 cells were exposed to LPS with or without 2-HB pretreatment (0.01–10.00 mmol·L^{-1}) [54]. The expression of tumor necrosis factor-α (TNF-α) was determined with quantitative real-time PCR (qRT-PCR). Our results showed that pretreatment with 2-HB significantly inhibited the LPS-induced up-regulation of TNF-α mRNA, which suggested that 2-HB inhibited inflammation (Fig. 4(a)). In addition, the effect of 2-HB on INS sensitivity was evaluated in HepG2 cells, which were treated with GS followed by INS stimulation with or without 2-HB pretreatment [55,56]. Our data showed that 2-HB pretreatment increased the ratios of p-insulin receptor (p-IR)/IR, p-insulin receptor substrate 1 (p-IRS1)/IRS1, and p-protein kinase B (p-AKT)/AKT in the context of GS cultivation, suggesting an improvement in INS sensitivity (Figs. 4(b)–(e)). Collectively, these results indicated that 2-HB stimulated lipolysis and improved INS sensitivity in hepatocytes, as well as reducing inflammation in macrophage cells.

3.4. 2-HB reduces serum TG levels and regulates lipid metabolism in HFHS-fed mice

Given the in vitro evidence of 2-HB on metabolic disorders, we next investigated the effects of orally administered 2-HB on lipids metabolism in a short-term HFHS-fed mouse. The final body weight after two weeks of HFHS feeding was higher than that in the control group, while no difference was observed between the HFHS and 2-HB groups (Fig. 5(a)). Interestingly, serum TG levels were significantly increased in the HFHS group but were reduced by 2-HB (Fig. 5(b)). In addition, there were no significant differences in the weight or index of the WAT or liver tissues between the HFHS and 2-HB groups, and no significant difference in the hepatic TG levels (Figs. 5(c)–(g)). The results of a glucose tolerance test (GTT) showed that the short-term intervention of 2-HB did not significantly improve the INS sensitivity of HFHS-fed mice (Fig. 6(a)).
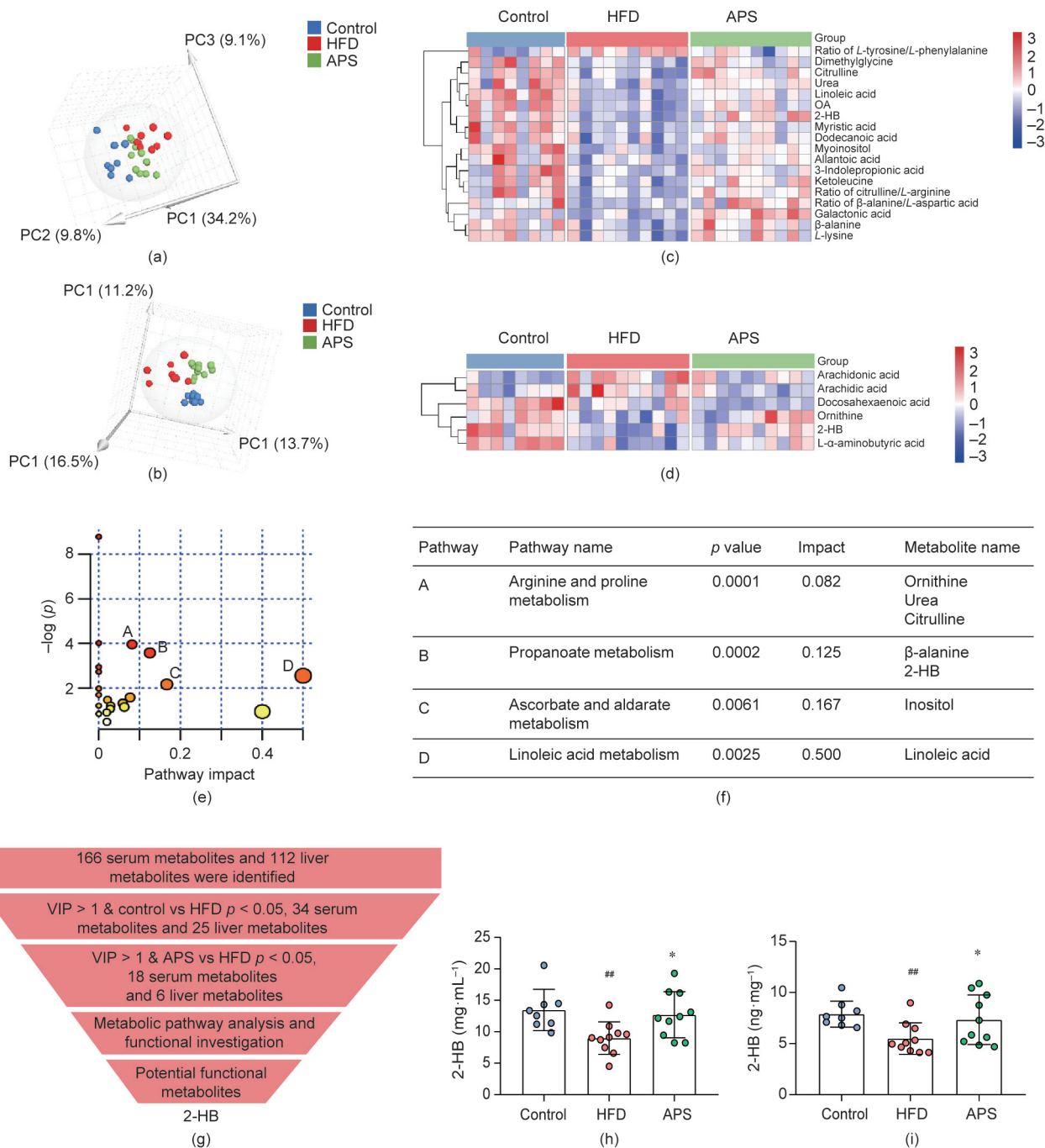
Fig. 2. Metabolomics reveals alteration of metabolic profiles and significant increases of 2-HB in APS-supplemented mice. Serum and liver samples were determined by GC–TOFMS; the untargeted metabolites in the study samples were annotated with the mammalian metabolite database JiaLib using a strict matching algorithm incorporated in XploreMET system. Next, the key metabolites that were obtained after screening was verified using LC–MS/MS. (a) Overview of the serum metabolic profiles of three groups using a three dimensional (3D)-PCA scores plot (n = 8, 10, and 10 per group). PC: principal component. (b) The differences in expression among the three groups of serum differential metabolites were visualized with a heatmap. (c) Overview of the liver metabolic profiles of the three groups using a 3D-PCA scores plot (n = 8, 10, and 10 per group). Red and blue entries indicate metabolites that showed respectively more and less expression in each sample. (d) The differences in expression among the three groups of liver differential metabolites were visualized with a heatmap. Red and blue entries indicate metabolites that showed respectively more and less expression in each sample. (e) Overview of pathway analysis; MetaboAnalyst was used to analyze the metabolic pathways on the KEGG website of the differential metabolites of APS-supplemented mice. (f) Differential metabolites contained in four metabolic pathways. (g) Selection of potential functional metabolites. Among the identified metabolites, metabolites that were significantly altered between groups (variable importance for the projection (VIP) > 1 and p < 0.05) were selected. To screen for differential metabolites associated with the role of APS in regulating lipid metabolism, metabolic pathway enrichment and a functional analysis were chosen. Expression of the selected key metabolite 2-HB in (h) serum and (i) liver was determined by targeted metabolomics LC–MS/MS. Significance was measured by an unpaired two-tailed Student's t-test, with $^{##}p$ < 0.01 compared to the control group and $^{*}p$ < 0.05 compared with HFD group. Results are presented as means ± SEM.

To further characterize whether 2-HB could modulate the lipids metabolism in mice, the mRNA or protein expression of the genes involved in lipids metabolism were investigated in the WAT and liver tissues, such as sterol-regulatory element-binding proteins (SREBP), fatty acid synthase (FAS), carbohydrate response element-binding protein (ChREBP), acetyl-CoA carboxylase (ACC), ATGL, HSL, CE1, and carnitine palmitoyltransferase-1 (CPT-1). We found that 2-HB treatment inhibited the HFHS-induced expression
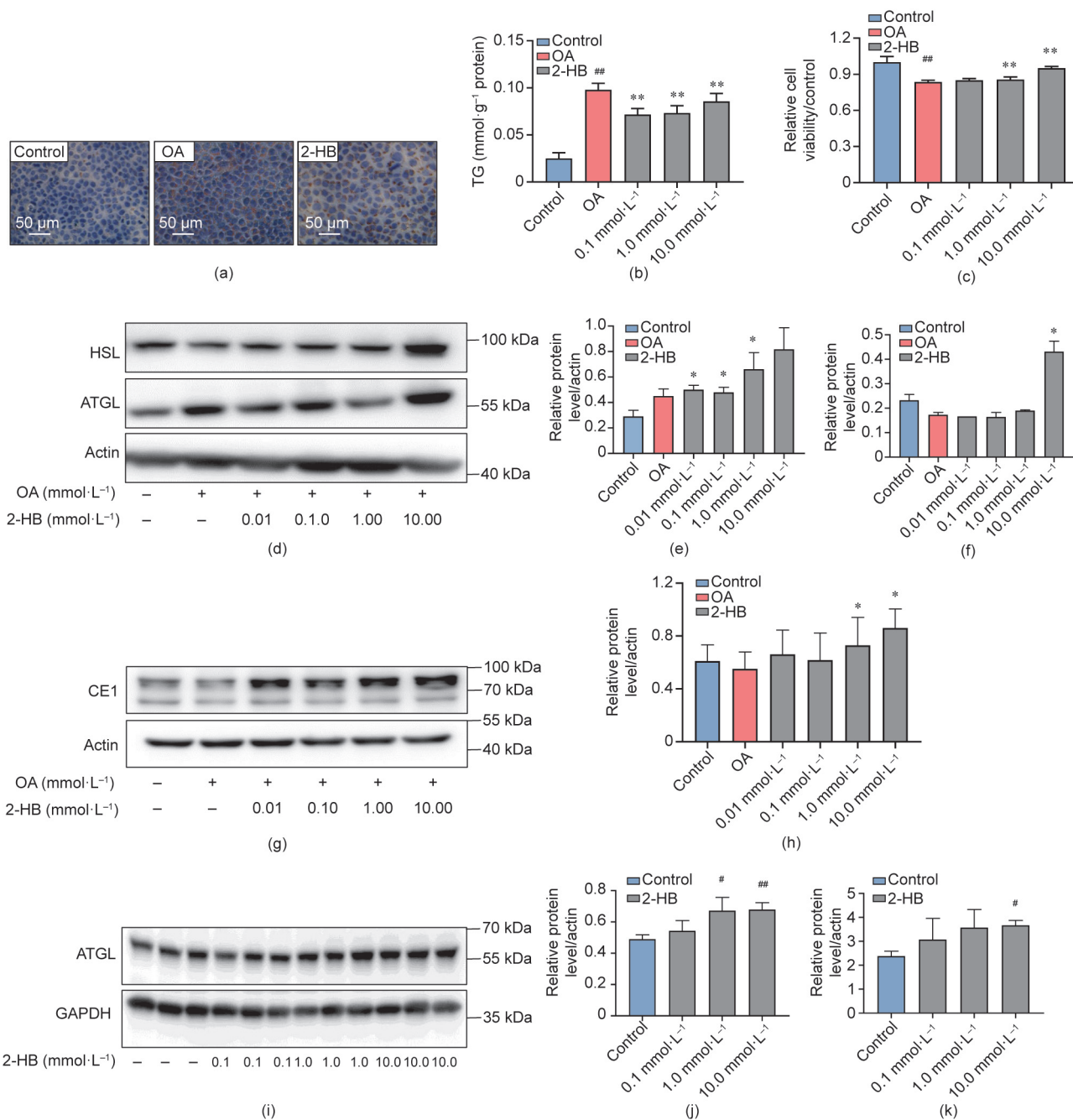
Fig. 3. 2-HB regulates lipid metabolism *in vitro*. *In vitro* experiments were designed to investigate the effect of 2-HB intervention on lipid metabolism. (a) Representative photomicrographs of AML12 cells with oil red O staining; cells were treated with 2-HB and OA for 24 h. (b) TG levels of AML12 cells after incubation with 2-HB and OA for 24 h (*n* = 4 per group). (c) Cell viability of AML12 cells after incubation with 2-HB and OA for 24 h (*n* = 6 per group). (d)–(h) Effect of 2-HB 24 h treatment on the protein expression of the lipid-degrading proteins HSL, ATGL, and CE1 on AML12 cells (*n* = 3–4 per group). (i) and (j) Effect of 2-HB 24 h treatment on ATGL protein expression on 3T3-L1 cells (*n* = 3 per group). (k) Glycerin levels on differentiated 3T3-L1 cells after treatment with 2-HB for 24 h (*n* = 3 per group). Significance was measured by an unpaired two-tailed Student's *t*-test, with #*p* < 0.05 and ##*p* < 0.01 compared with the control group, and *p* < 0.05 and **p* < 0.01 compared with the OA group. Results are presented as means ± SEM.

of genes or proteins in WAT, including the mRNA of FAS and ACC, and the proteins of SREBP and FAS (Figs. 6(b)–(e)). In contrast, 2-HB treatment increased the expression of ATGL and HSL proteins in WAT (Figs. 6(f)–(h)). Meanwhile, HFHS feeding resulted in suppression of CE1 and up-regulation of SREBP and FAS proteins in liver tissues, all of which were obviously reversed by 2-HB treatment (Figs. 6(i)–(k)).

We further tested the effects of 2-HB on lipids metabolism by means of a two-week intraperitoneal injection in HFHS-fed mice. In line with the results of oral administration, the data showed that 2-HB injection reduced serum TG levels and reversed the expression of SREBP, FAS, and CE1 proteins in liver tissues, albeit with no effect on body weight gain (Appendix A Fig. S5).

Taken together, these results indicated that the metabolite 2-HB resulting from APS treatment was effective in modulating lipids metabolism and INS sensitivity both *in vitro* and *in vivo*, which might contribute to the metabolic benefits of APS.
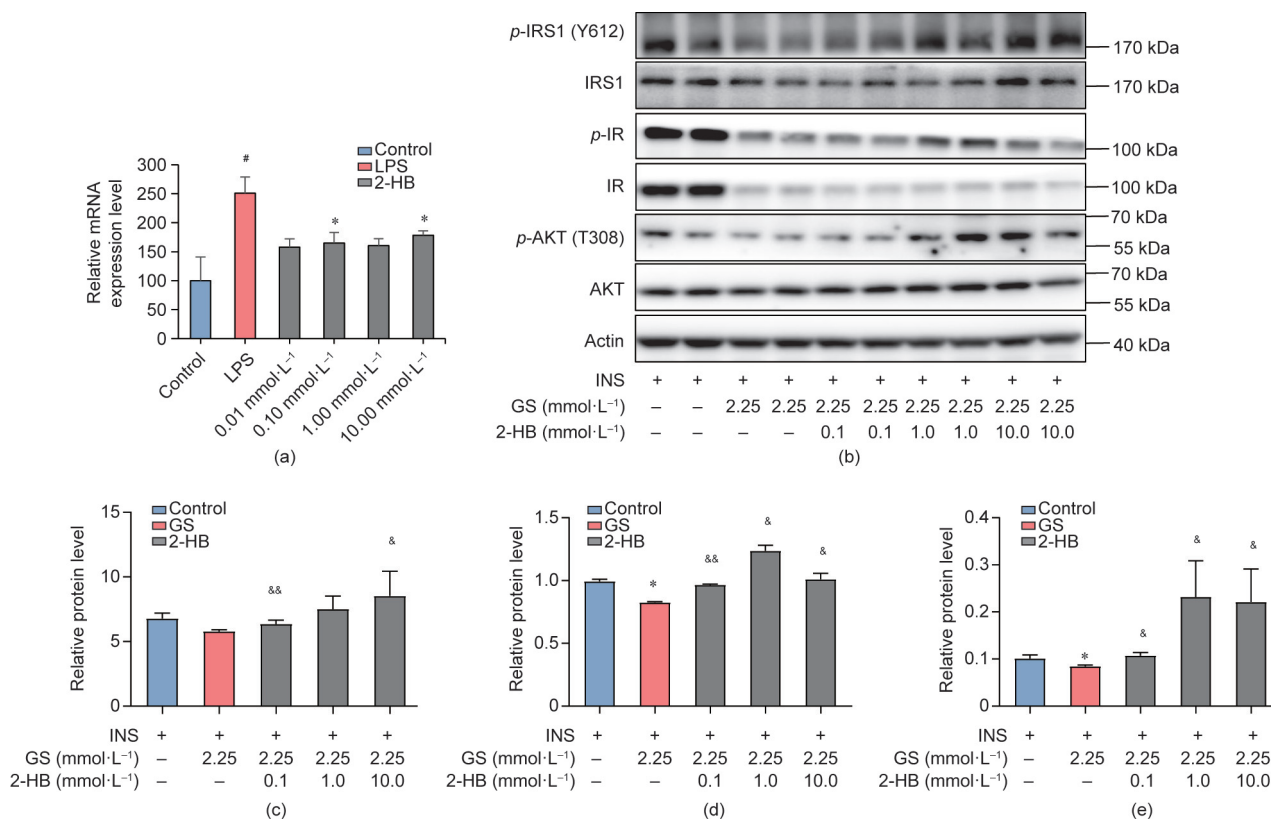
Fig. 4. 2-HB suppresses inflammation levels and enhances INS sensitivity *in vitro*. The inflammatory model and INS resistance model were established on macrophage RAW264.7 and human hepatocyte HepG2, respectively. (a) The mRNA expression level of pro-inflammatory cytokine TNF-α on RAW264.7 cells with 2-HB and LPS intervention (n = 4 per group). (b) The phosphorylated and total protein expression level of IRS1, IR, and AKT on HepG2 cells with 2-HB, GS, and INS intervention were detected. (c)–(e) The ratios of IRS1, IR, and AKT phosphorylated protein to total protein on HepG2 cells (n = 4 per group). Significance was measured by an unpaired two-tailed Student's *t*-test, with #$p < 0.05$ compared with the control group, *$p < 0.05$ compared with INS or LPS group, and &$p < 0.05$ and &&$p < 0.01$ compared with GS group. Results are presented as means ± SEM.
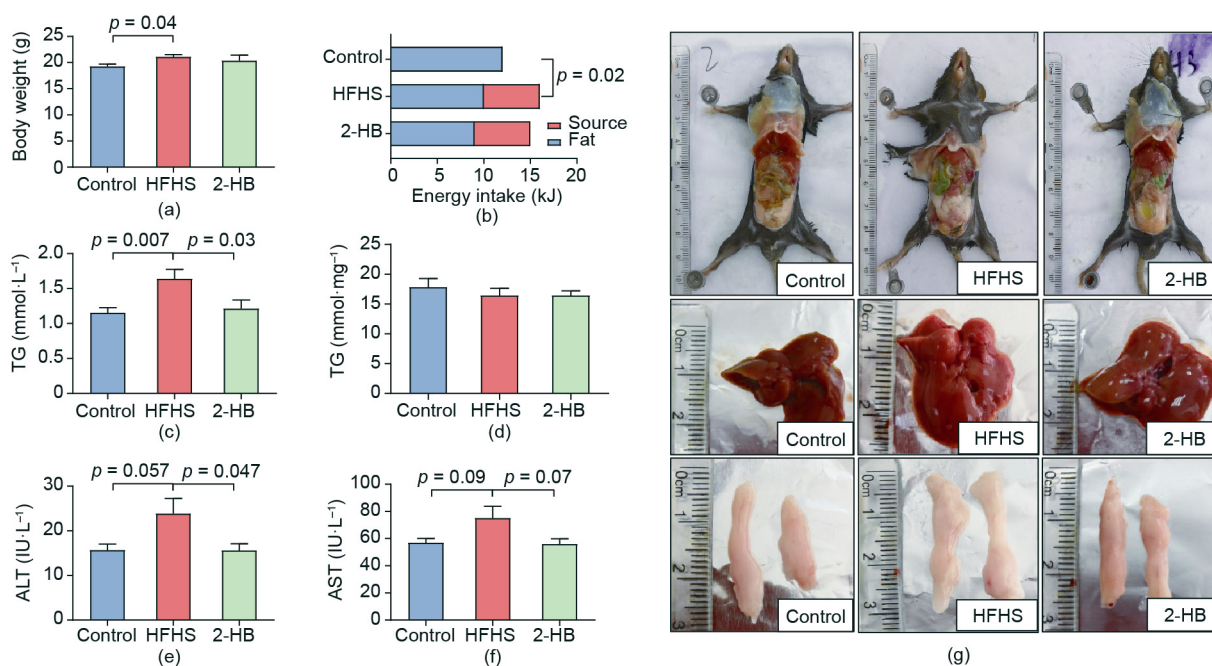
Fig. 5. 2-HB regulates serum lipid level and liver damage in HFHS-fed mice. Male C57BL/6J mice (four weeks old) were treated with a chow diet (control) or a HFHS (30% sucrose supplementation in water, g·L⁻¹) diet with or without 250 mg·kg⁻¹ 2-HB intervention by stomach perfusion for two weeks. (a) Body weight at the end of the experiment (n = 10, 12, and 10 per group). (b) Energy intake (n = 10, 12, and 10 per group). (c) Serum TG levels (n = 10, 12, and 10 per group). (d) Liver TG levels (n = 8, 10, and 10 per group). (e) and (f) Serum ALT and AST levels (n = 8, 10, and 9 per group). IU: international unit. (g) Mice body, liver, and WAT. Significance was measured by an unpaired two-tailed Student's *t*-test. Results are presented as means ± SEM.
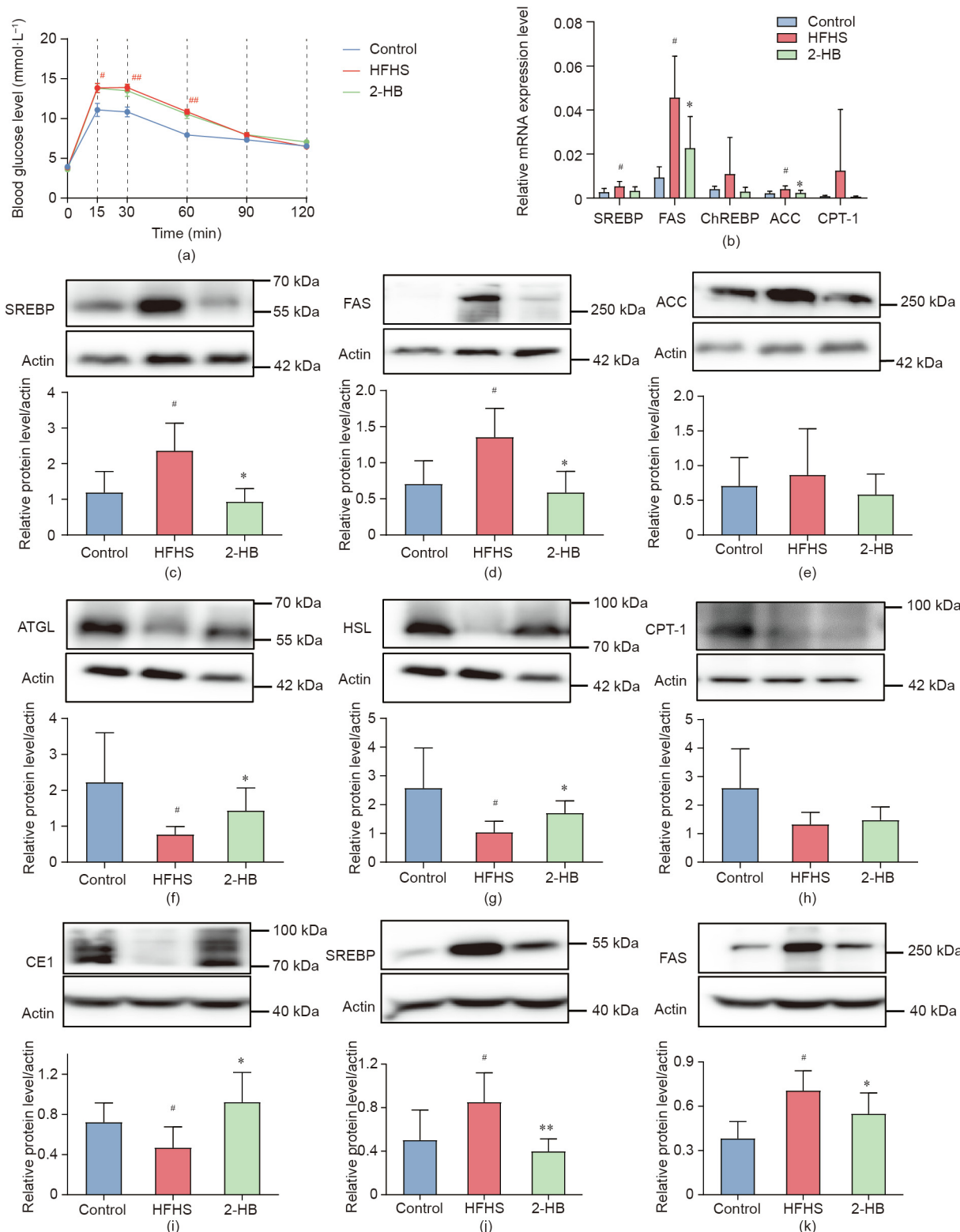
Fig. 6. 2-HB regulates lipid metabolism in HFHS-fed mice. Male C57BL/6J mice (four weeks old) were treated with a chow diet (control), or a HFHS (30% sucrose supplementation in water, g·L^{-1}) diet with or without 250 mg·kg^{-1} 2-HB intervention by intraperitoneal injection for two weeks. (a) GTT curve (n = 6, 10, and 9 per group). (b) The mRNA expression levels of SREBP, FAS, ChREBP, ACC, and CPT-1 in WAT (n = 10, 6, and 10 per group). (c)–(h) Protein expression levels of SREBP, FAS, ACC, ATGL, HSL, and CPT-1 in WAT (n = 4–7 per group). (i)–(k) Protein expression levels of CE1, SREBP, and FAS in liver tissues (n = 6–9 per group). Significance was measured by an unpaired two-tailed Student's t-test, with $^{\#}p < 0.05$ and $^{\#\#}p < 0.01$ compared with the control group, and $^{*}p < 0.05$ and $^{**}p < 0.01$ compared with the HFHS group. Results are presented as means ± SEM.

4. Discussion

This study indicated that APS is effective in improving metabolic disorders in obese mice by reducing body weight gain, attenuating hepatic steatosis, and decreasing adiposity. Furthermore, untargeted and targeted metabolomics revealed that APS supplementation resulted in an increase of 2-HB in serum and liver tissues. We further demonstrated that 2-HB can modulate mRNA or the protein expression of the genes involved in fatty acid metabolism, inhibit inflammation, and improve INS sensitivity in HepG2 or 3T3-L1 cells; it also reduces serum TG and lipids metabolism in HFHS-fed mice.

The metabolic benefits of most plant polysaccharides are well established. The mechanisms underlying the protective effect of polysaccharides are mainly recognized to be associated with modulation of the gut microbiota [57], because of the non-absorption of such polysaccharides in the gastrointestinal tract [58]. However, the exact metabolism improved mechanisms of plant polysaccharides are not well understood. Our previous observations indicated that the anti-obesity effect of APS was associated with modulation of the gut microbiota [19]. Moreover, we found that APS did not inhibit TG accumulation in OA-treated HepG2 cells (data not shown), which excluded the possibility of the direct action of APS on lipids metabolism.

Increasing evidence has shown that endogenous or microbiota-derived metabolites usually perform vital functions in maintaining health, disease development, and drug activity [59–61]. Changes in metabolites are not only readouts of a disturbance occurring at the gene or protein level; they also serve as signaling molecules to modulate the pathophysiological status [62]. Therefore, functional metabolomics is extremely valuable for investigating the potential functions of identified differential metabolites [63]. Since the mechanisms underlying the metabolic benefits of most plant polysaccharides, including APS, are largely unclear, we adopted untargeted metabolomics to investigate whether the metabolic benefits of APS were associated with modulation of the endogenous metabolism. The metabolomics results showed that APS supplementation obviously restored the metabolic changes induced by HFD in both serum and liver tissues, which suggests that the metabolic benefits of APS are probably associated with modulation of the host metabolism. Further analysis revealed 18 and 6 differential metabolites in serum and liver tissues, respectively, that were reversely altered by an HFD or APS supplementation. More than half of the differential metabolites are amino acids, which may have functions within the host such as regulating cellular signals, gene expression, acting as building blocks for protein synthesis or phosphorylation, or enabling hormone synthesis [64].

To determine the metabolites that may be associated with the activity of APS, we performed metabolic pathway enrichment with the 24 identified metabolites (18 from serum and 6 from liver tissues) and literature research. We then obtained four main metabolic pathways that were significantly altered by HFD and APS supplementation, including the pathways of arginine and proline metabolism, propanoate metabolism, linoleic acid metabolism, and ascorbate and aldarate metabolism. We paid a great deal of attention to the propanoate metabolism pathway containing beta-alanine and 2-HB, because this pathway had low p values and high pathway impacts, in addition to the well-established roles of short-chain fatty acids, which containing propionic acid, in metabolic diseases [65,66]. The metabolite 2-HB was selected based on the following reasons: First of all, the chemical structure of 2-HB is similar to that of β-HB and butyric acid, which have important functions in affecting the development of metabolic diseases [67,68]. Second, although increased levels of 2-HB have been observed in patients with diabetes, obesity, or metabolic syndromes, which suggests that 2-HB is probably a biomarker for

metabolic syndrome or diabetes [69,70], the biological functions of 2-HB in metabolic diseases are unclear. Third, in addition to the endogenous origin of 2-HB from precursors such as 3-HB, 2-aminobutyric acid, α-ketobutyric acid, 2-oxobutyric acid, and amino acids including methionine, threonine, and homoserine [71,72], 2-HB could be produced by bacteria through lactate dehydrogenase (LDH) enzymes [73–77]. In addition, our previous study observed that alteration of the gut microbiota with vancomycin increased the production of 2-HB [78]. Given the fact of gut microbiota modulation by APS supplementation [19], we considered that the metabolic benefits of APS supplementation might be associated with the production of 2-HB. Although we cannot clearly determine the origin of 2-HB in the current study, the increased production of 2-HB in APS-supplemented mice may be derived from either the host metabolism or the gut microbiota in the context of modulation of the gut microbiota by APS.

Dysregulated lipids metabolism is the basis for the development of metabolic diseases [79]. A previous study indicated that 2-HB could inhibit lipid synthesis in the cerebral cortex of rats [80]. Proteins of ATGL and HSL catalyze the hydrolysis of TG mainly in adipocytes, and in hepatocytes as well [81], whereas CE1 is specifically expressed in hepatocytes for TG hydrolysis [82]. Our in vitro experiment indicated that 2-HB stimulated the expression of HSL, ATGL, and CE1 proteins in hepatocytes and glycerin release in 3T3-L1 cells, suggesting enhanced lipids degradation by 2-HB.

INS resistance and inflammation are important risk factors of metabolic diseases [53,83–86]. 2-HB treatment inhibited the expression of pro-inflammatory cytokine TNF-α in macrophages, and improved INS sensitivity in hepatocytes. The in vitro results suggested that 2-HB might be beneficial for attenuating metabolic disorders. No significant differences were observed in the weight or index of WAT and liver tissues, or in the TG levels in liver tissues, between the 2-HB and HFHS groups. However, the results showed that either intragastric or intraperitoneal injection of 2-HB for two weeks could reduce serum TG level, inhibit the expression of FAS and SREBP proteins, and stimulate ATGL, HSL, and CE1 expression in WAT and liver tissues in HFHS-fed mice. The in vitro and in vivo results suggest that 2-HB was effective in modulating lipids metabolism, especially in regulating the expression of the key genes at the mRNA or protein level that are involved in fatty acid synthesis or lipolysis. It should be noted that the biological functions of 2-HB were only tested in short-term HFHS-fed mice in the current study, in which the mice were characterized by an obvious increase of serum TG, instead of hepatic TG levels. It was found that 2-HB reduced the TG levels in the serum and reversed the expression of genes and proteins that are critically involved in lipids metabolism in WAT or liver tissues of HFHS-fed mice after a two-week intervention. Although we did not observe the reduction of hepatic TG after two weeks of 2-HB treatment, the significant modulation of the expression of the genes and proteins that are critically involved in fatty acid synthesis and oxidation suggested that more comprehensive effects of 2-HB on lipids metabolism could be expected if a long-term intervention of 2-HB was performed.

In conclusion, this study confirms the metabolic benefits of APS in HFD-fed mice and identifies a functional metabolite, 2-HB, that is increased in serum and liver tissues by APS supplementation. Further investigation revealed that 2-HB modulates lipids metabolism both in vitro and in vivo, especially by inhibiting or stimulating the expression of proteins involved in de novo fatty acid synthesis or lipid degradation. Our results suggest that the metabolic benefits of APS in HFD-fed mice may at least partially occur through the production of 2-HB in mice. Further investigation is warranted to confirm the functions of 2-HB in long-term HFD-fed animals, and to determine the exact origin of 2-HB in APS-supplemented mice.

Acknowledgments

Authors' contribution

Bingbing Li performed all of the *in vitro* experiments and wrote the manuscript. Ying Hong performed animal experimentation for the APS supplementation study and untargeted metabolomics. Yu Gu conducted targeted metabolomics and data analysis. Shengjie Ye helped with the *in vitro* experiment. Jian Yao and Kan Ding analyzed the monosaccharide composition of *Astragalus* polysaccharides. Kaili Hu helped in the study design. Aihua Zhao and Wei Jia helped with the untargeted metabolomics. Houkai Li supervised the project and revised the manuscript. All the authors approved the final version of this manuscript.

Compliance with ethics guidelines

Bingbing Li, Ying Hong, Yu Gu, Shengjie Ye, Kaili Hu, Jian Yao, Kan Ding, Aihua Zhao, Wei Jia, and Houkai Li declare that they have no conflict of interest or financial conflicts to disclose.

Appendix A. Supplementary data

Supplementary data to this article can be found online at https://doi.org/10.1016/j.eng.2020.05.023.

References

[1] Ford ES, William WHG. Prevalence of the metabolic syndrome among US adults. JAMA Cardiol 2002;287(3):356–9.
[2] Jensen MD, Caruso M, Heiling V, Miles JM. Insulin regulation of lipolysis in nondiabetic and IDDM subjects. Diabetes 1989;38(12):1595–601.
[3] Weiss R, Dziura J, Burgert TS, Tamborlane WV, Taksali SE, Yeckel CW, et al. Obesity and the metabolic syndrome in children and adolescents. New Engl J Med 2004;350:2362–74.
[4] Robert HE, Scott MG, Zimmet PZ. The metabolic syndrome. Lancet 2005;365 (9468):1415–28.
[5] Lewis GF, Uffelman KD, Szeto LW, Weller B, Steiner G. Interaction between free fatty acids and insulin in the acute control of very low density lipoprotein production in humans. J Clin Invest 1995;1(95):158–66.
[6] McCarthy EM, Rinella ME. The role of diet and nutrient composition in nonalcoholic fatty liver disease. J Acad Nutr Diet 2012;112(3):401–9.
[7] Cohen JC, Horton JD, Hobbs HH. Human fatty liver disease: old questions and new insights. Science 2011;332(6037):1519–23.
[8] Younossi ZM. Non-alcoholic fatty liver disease—a global public health perspective. J Hepatol 2019;70(3):531–44.
[9] Narayanaswami V, Dwoskin LP. Obesity: current and potential pharmacotherapeutics and targets. Pharmacol Therapeut 2017;170:116–47.
[10] Chan K, Zhang H, Lin Z. An overview on adverse drug reactions to traditional Chinese medicines. Br J Clin Pharmacol 2015;80(4):834–43.
[11] Lu Y, Jiang Y, Ling L, Zhang Y, Li H, Chen D. Beneficial effects of *Houttuynia cordata* polysaccharides on "two-hit" acute lung injury and endotoxic fever in rats associated with anti-complementary activities. Acta Pharm Sin B 2018;8 (2):218–27.
[12] Chang C, Lin C, Lu C, Martel J, Ko Y, Ojcius DM, et al. Ganoderma lucidum reduces obesity in mice by modulating the composition of the gut microbiota. Nat Commun 2015;6(1):7489.
[13] Wu T, Lin C, Chang C, Lin T, Martel J, Ko Y, et al. Gut commensal *Parabacteroides goldsteinii* plays a predominant role in the anti-obesity effects of polysaccharides isolated from *Hirsutella sinensis*. Gut 2019;68(2):248–62.
[14] Fu J, Wang Z, Huang L, Zheng S, Wang D, Chen S, et al. Review of the botanical characteristics, phytochemistry, and pharmacology of *Astragalus membranaceus* (Huangqi). Phytother Res 2014;28(9):1275–83.
[15] Liu P, Zhao H, Luo Y. Anti-aging implications of *Astragalus membranaceus* (Huangqi): a well-known Chinese tonic. Aging Dis 2017;8(6):868–86.
[16] Mao X, Yu F, Wang N, Wu Y, Zou F, Wu K, et al. Hypoglycemic effect of polysaccharide enriched extract of *Astragalus membranaceus* in diet induced insulin resistant C57BL/6J mice and its potential mechanism. Phytomedicine 2009;16(5):416–25.
[17] Huang Y, Tsay H, Lu M, Lin C, Yeh C, Liu H, et al. *Astragalus membranaceus*-polysaccharides ameliorates obesity, hepatic steatosis, neuroinflammation and cognition impairment without affecting amyloid deposition in metabolically stressed APPswe/PS1dE9 mice. Int J Mol Sci 2017;18 (12):2746–63.
[18] Liu M, Qin J, Hao Y, Liu M, Luo J, Luo T, et al. *Astragalus polysaccharide* suppresses skeletal muscle myostatin expression in obesity: involvement of ROS-ERK and NF-κB pathways. Oxid Med Cell Longev 2013;2013:1–10.
[19] He X, He J, Zheng N, Wang S, Li H. Study on the relationship between weight reduction and intestinal bacterial regulation of *Astragalus polysaccharide* in obese mice. World J Tradit Chin Med 2016;11(11):2379–84.
[20] Newgard CB. Metabolomics and metabolic diseases: where do we stand? Cell Metab 2017;25(1):43–56.
[21] Chávez-Talavera O, Tailleux A, Lefebvre P, Staels B. Bile acid control of metabolism and inflammation in obesity, type 2 diabetes, dyslipidemia, and nonalcoholic fatty liver disease. Gastroenterology 2017;7(152):1679–94.
[22] Lampropoulou V, Sergushichev A, Bambouskova M, Nair S, Vincent EE, Loginicheva E, et al. Itaconate links inhibition of succinate dehydrogenase with macrophage metabolic remodeling and regulation of inflammation. Cell Metab 2016;24(1):158–66.
[23] McNabney S, Henagan T. Short chain fatty acids in the colon and peripheral tissues: a focus on butyrate, colon cancer, obesity and insulin resistance. Nutrients 2017;9(12):1348.
[24] Koh GY, Chou G, Liu Z. Purification of a water extract of Chinese sweet tea plant (*Rubus suavissimus* S. Lee) by alcohol precipitation. J Agric Food Chem 2009;57(11):5000–6.
[25] Lin L, Wang P, Du Z, Wang W, Cong Q, Zheng C, et al. Structural elucidation of a pectin from flowers of *Lonicera japonica* and its antipancreatic cancer activity. Int J Biol Macromol 2016;88:130–7.
[26] Ni Y, Su M, Qiu Y, Jia W, Du X. ADAP-GC 3.0: improved peak detection and deconvolution of co-eluting metabolites from GC/TOF-MS data for metabolomics studies. Anal Chem 2016;88(17):8802–11.
[27] Gijs Den B, Aycha B, Albert G, Karen Van E, Rick H, Theo H, et al. Short-chain fatty acids protect against high-fat diet-induced obesity via a PPARγ-dependent switch from lipogenesis to fat oxidation. Diabetes 2015;64:2398–408.
[28] Whelan J, Fritsche K. Linoleic acid. Adv Nutr 2013;4(3):311–2.
[29] Gooda Sahib Jambocus N, Saari N, Ismail A, Khatib A, Mahomoodally MF, Abdul HA. An investigation into the antiobesity effects of *Morinda citrifolia* L. leaf extract in high fat diet induced obese rats using a ^{1}H NMR metabolomics approach. J Diabetes Res 2016;2016:1–14.
[30] Drenick EJ, Alvarez LC, Tamasi GC, Brickman AS. Resistance to symptomatic insulin reactions after fasting. J Clin Invest 1972;51(10):2757–62.
[31] Werner E, Froehlich R. The potential role for myoinositol in the prevention of gestational diabetes mellitus. Am J Perinatol 2016;13(33):1236–41.
[32] Araya J, Rodrigo R, Videla LA, Thielemann L, Orellana M, Pettinelli P, et al. Increase in long-chain polyunsaturated fatty acid n–6/n–3 ratio in relation to hepatic steatosis in patients with non-alcoholic fatty liver disease. Clin Sci 2004;106(6):635–43.
[33] Wada Y, Sakiyama S, Sakai H, Sakane F. Myristic acid enhances diacylglycerol kinase δ-dependent glucose uptake in myotubes. Lipids 2016;51(8):897–903.
[34] Magnusson M, Wang TJ, Clish C, Engström G, Nilsson P, Gerszten RE, et al. Dimethylglycine deficiency and the development of diabetes. Diabetes 2015;64:3010–6.
[35] Carvalho VH, Oliveira AHS, de Oliveira LF, Da Silva RP, Di Mascio P, Gualano B, et al. Exercise and β-alanine supplementation on carnosine–acrolein adduct in skeletal muscle. Redox Biol 2018;18:222–8.
[36] Saitoh W, Takada S, Hirao J, Shirai M, Iguchi T, Tsuji M, et al. Plasma citrulline is a sensitive safety biomarker for small intestinal injury in rats. Toxicol Lett 2018;295:416–23.
[37] Wei P, Rui T, Ruilan W. Clinical application of plasma citrulline in intestinal damage. J Clin Emerg Med 2018;04(19):274–8.
[38] Elliott P, Posma JM, Chan Q, Garcia-Perez I, Wijeyesekera A, Bictash M, et al. Urinary metabolic signatures of human adiposity. Sci Transl Med 2015;7 (285):285ra62.
[39] Judith LF, Peter AS, Joseph V, Mark DW, Qian G. Role of carnitine in disease. Nutr Metab 2010;7:30.
[40] Zhang LS, Davies SS. Microbial metabolism of dietary components to bioactive metabolites: opportunities for new therapeutic interventions. Genome Med 2016;8(1):46.
[41] Wikoff WR, Anfora AT, Liu J, Schultz PG, Lesley SA, Peters EC, et al. Metabolomics analysis reveals large effects of gut microflora on mammalian blood metabolites. Proc Natl Acad Sci USA 2009;106(10):3698–703.
[42] Traynor J, Mactier R, Geddes CC, Fox JG. How to measure renal function in clinical practice. BMJ 2006;333(7571):733–7.
[43] Mensink RP, Zock PL, Kester AD, Katan MB. Effects of dietary fatty acids and carbohydrates on the ratio of serum total to HDL cholesterol and on serum lipids and apolipoproteins: a meta-analysis of 60 controlled trials. Am J Clin Nutr 2003;77(5):1146–55.
[44] Mohnen D. Pectin structure and biosynthesis. Curr Opin Plant Biol 2008;11 (3):266–77.
[45] Irino Y, Toh R, Nagao M, Mori T, Honjo T, Shinohara M, et al. 2-Aminobutyric acid modulates glutathione homeostasis in the myocardium. Sci Rep 2016;1 (6):36749.
[46] Arthur L, Weber I, Stanley LM, Abdul HA. Reasons for the occurrence of the twenty coded protein amino acid. J Mol Evol 1981;17:273–84.

[47] Nelson GJ, Schmidt PC, Bartolini G, Kelley DS, Kyle D. The effect of dietary arachidonic acid on platelet function, platelet fatty acid composition, and blood coagulation in humans. Lipids 1997;32(4):421–5.

[48] Ferrucci L, Cherubini A, Bandinelli S, Bartali B, Corsi A, Lauretani F, et al. Relationship of plasma polyunsaturated fatty acids to circulating inflammatory markers. J Clin Endocrinol Metab 2006;91(2):439–46.

[49] Yan C, Yusha W, Bing W. Research progress on the neuroprotective effect of docosahexaenoic acid. Pract Med Clin 2015;06(18):721–4.

[50] Bell M, Wang H, Chen H, McLenithan JC, Gong DW, Yang RZ, et al. Consequences of lipid droplet coat protein downregulation in liver cells: abnormal lipid droplet metabolism and induction of insulin resistance. Diabetes 2008;57(8):2037–45.

[51] Hsiao P, Chiou HC, Jiang H, Lee M, Hsieh T, Kuo K. Pioglitazone enhances cytosolic lipolysis, β-oxidation and autophagy to ameliorate hepatic steatosis. Sci Rep 2017;1(7):9030.

[52] He W, Xu Y, Ren X, Xiang D, Lei K, Zhang C, et al. Vitamin E ameliorates lipid metabolism in mice with nonalcoholic fatty liver disease via Nrf2/CES1 signaling pathway. Dig Dis Sci 2019;64(11):3182–91.

[53] Odegaard JI, Chawla A. Pleiotropic actions of insulin resistance and inflammation in metabolic homeostasis. Science 2013;339(6116):172–7.

[54] Yang SZQQ. MicroRNA-124 negatively regulates LPS-induced TNF-α production in mouse macrophages by decreasing protein stability. Chin J Pharmacol 2016;7(37):889–97.

[55] Zhu D, Wang Y, Du Q, Liu Z, Liu X. Cichoric acid reverses insulin resistance and suppresses inflammatory responses in the glucosamine-induced HepG2 cells. J Agric Food Chem 2015;63(51):10903–13.

[56] Mi Y, Qi G, Gao Y, Li R, Wang Y, Li X, et al. (−)-Epigallocatechin-3-gallate ameliorates insulin resistance and mitochondrial dysfunction in HepG2 cells: involvement of Bmal1. Mol Nutr Food Res 2017;12(61):1700440.

[57] Wu T, Lin C, Chang C, Lin T, Martel J, Ko Y, et al. Gut commensal Parabacteroides goldsteinii plays a predominant role in the anti-obesity effects of polysaccharides isolated from Hirsutella sinensis. Gut 2019;2(68):248–62.

[58] Porter NT, Martens EC. The critical roles of polysaccharides in gut microbial ecology and physiology. Annu Rev Microbiol 2017;1(71):349–69.

[59] Ussher JR, Elmariah S, Gerszten RE, Dyck JRB. The emerging role of metabolomics in the diagnosis and prognosis of cardiovasculat disease. J Am Coll Cardiol 2016;25(68):2850–70.

[60] Lampropoulou V, Sergushichev A, Bambouskova M, Nair S, Vincent EE, Loginicheva E, et al. Itaconate links inhibition of succinate dehydrogenase with macrophage metabolic remodeling and regulation of inflammation. Cell Metab 2016;1(24):158–66.

[61] Garaycoechea JI, Crossan GP, Langevin F, Daly M, Arends MJ, Patel KJ. Genotoxic consequences of endogenous aldehydes on mouse haematopoietic stem cell function. Nature 2012;7417(489):571–5.

[62] Chin RM, Fu X, Pai MY, Vergnes L, Hwang H, Deng G, et al. The metabolite α-ketoglutarate extends lifespan by inhibiting ATP synthase and TOR. Nature 2014;510(7505):397–401.

[63] Min Y, Guowang X. Current and future perspectives of functional metabolomics in disease studies—a review. Anal Chim Acta 2018;1037:41–54.

[64] Wu G. Amino acids: metabolism, functions, and nutrition. Amino Acids 2009;37(1):1–17.

[65] Chambers ES, Byrne CS, Morrison DJ, Murphy KG, Preston T, Tedford C, et al. Dietary supplementation with inulin-propionate ester or inulin improves insulin sensitivity in adults with overweight and obesity with distinct effects on the gut microbiota, plasma metabolome and systemic inflammatory responses: a randomised cross-over trial. Gut 2019;68(8):1430–8.

[66] Chambers ES, Viardot A, Psichas A, Morrison DJ, Murphy KG, Zac-Varghese SEK, et al. Effects of targeted delivery of propionate to the human colon on appetite regulation, body weight maintenance and adiposity in overweight adults. Gut 2015;64(11):1744–54.

[67] Newman JC, Verdin E. β-Hydroxybutyrate: a signaling metabolite. Annu Rev Nutr 2017;37(1):51–76.

[68] Zhou D, Chen YW, Zhao ZH, Yang RX, Xin FZ, Liu XL, et al. Sodium butyrate reduces high-fat diet-induced non-alcoholic steatohepatitis through upregulation of hepatic GLP-1R expression. Exp Mol Med 2018;50(12):157.

[69] Ferrannini E, Natali A, Camastra S, Nannipieri M, Mari A, Adam KP, et al. Early metabolic markers of the development of dysglycemia and type 2 diabetes and their physiological significance. Diabetes 2013;62(5):1730–7.

[70] Lin Z, Vicente Gonçalves CM, Dai L, Lu H, Huang J, Ji H, et al. Exploring metabolic syndrome serum profiling based on gas chromatography mass spectrometry and random forest models. Anal Chim Acta 2014;827:22–7.

[71] Landaas S. The formation of 2-hydroxybutyric acid in experimental animals. Clin Chim Acta 1975;58(1):23–32.

[72] Adams SH. Emerging perspectives on essential amino acid metabolism in obesity and the insulin-resistant state. Adv Nutr 2011;2(6):445–56.

[73] Chaillou S, Champomier-Vergès M, Cornet M, Crutz-Le Coq A, Dudez A, Martin V, et al. The complete genome sequence of the meat-borne lactic acid bacterium Lactobacillus sakei 23K. Nat Biotechnol 2005;23(12):1527–33.

[74] Gao C, Zhang W, Ma C, Liu P, Xu P. Kinetic resolution of 2-hydroxybutanoate racemic mixtures by NAD-independent l-lactate dehydrogenase. Bioresour Technol 2011;102(7):4595–9.

[75] Heidelberg JF, Seshadri R, Haveman SA, Hemme CL, Paulsen IT, Kolonay JF, et al. The genome sequence of the anaerobic, sulfate-reducing bacterium Desulfovibrio vulgaris Hildenborough. Nat Biotechnol 2004;22 (5):554–9.

[76] Kapatral V, Anderson I, Ivanova N, Reznik G, Los T, Lykidis A, et al. Genome sequence and analysis of the oral bacterium Fusobacterium nucleatum strain ATCC 25586. J Bacteriol 2002;184(7):2005–18.

[77] Monot M, Boursaux-Eude C, Thibonnier M, Vallenet D, Moszer I, Medigue C, et al. Reannotation of the genome sequence of Clostridium difficile strain 630. J Med Microbiol 2011;60(Pt 8):1193–9.

[78] Zheng N, Gu Y, Hong Y, Sheng L, Chen L, Zhang F, et al. Vancomycin pretreatment attenuates acetaminophen-induced liver injury through 2-hydroxybutyric acid. J Pharm Anal. In press.

[79] Savage DB, Petersen KF, Shulman GI. Disordered lipid metabolism and the pathogenesis of insulin resistance. Physiol Rev 2007;87(2):507–20.

[80] Silva AR, Ruschel C, Helegda C, Wyse AT, Wannmacher CM, Wajner M, et al. Inhibition of in vitro CO$_2$ production and lipid synthesis by 2-hydroxybutyric acid in rat brain. Braz J Med Biol Res 2001;34(5):627–31.

[81] Schott MB, Rasineni K, Weller SG, Schulze RJ, Sletten AC, Casey CA, et al. β-Adrenergic induction of lipolysis in hepatocytes is inhibited by ethanol exposure. J Biol Chem 2017;292(28):11815–28.

[82] Quiroga AD, Li L, Trötzmüller M, Nelson R, Proctor SD, Köfeler H, et al. Deficiency of carboxylesterase 1/esterase-x results in obesity, hepatic steatosis, and hyperlipidemia. Hepatology 2012;56(6):2188–98.

[83] Eizirik DL, Colli ML, Ortis F. The role of inflammation in insulitis and β-cell loss in type 1 diabetes. Nat Rev Endocrinol 2009;5(4):219–26.

[84] Glass CK, Olefsky JM. Inflammation and lipid signaling in the etiology of insulin resistance. Cell Metab 2012;15(5):635–45.

[85] Lee HY, Birkenfeld AL, Jornavaz FR, Jurczak MJ, Kanda S, Popov V, et al. Apolipoprotein CIII overexpressing mice are predisposed to diet-induced hepatic steatosis and hepatic insulin resistance. Hepatology 2011;54 (5):1650–60.

[86] Shoelson SE. Inflammation and insulin resistance. J Clin Invest 2006;116 (7):1793–801.